International Journal of Engineering and Advanced Technology (IJEAT)
ISSN: 2249–8958, Volume-1 Issue-3, February 2012

Iris Recognition - An Efficient Biometric for Human Identification and Verification

Ashish Kumar Dewangan, Majid Ahmed Siddhiqui

Abstract: ***A biometric system provides automatic identification of an individual based on a unique feature or characteristic possessed by the individual. Iris recognition is regarded as the most reliable and accurate biometric identification system available. Most commercial iris recognition systems use patented algorithms developed by Daugman, and these algorithms are able to produce perfect recognition rates. However, published results have usually been produced under favorable conditions, and there have been no independent trials of the technology. The work presented in this paper involved developing an 'open-source' iris recognition system in order to verify both the uniqueness of the human iris and also its performance as a biometric. For determining the recognition performance of the system one databases of digitized grayscale eye images were used. The iris recognition system consists of an automatic segmentation system that is based on the Hough transform, and is able to localize the circular iris and pupil region, occluding eyelids and eyelashes, and reflections. The extracted iris region was then normalized into a rectangular block with constant dimensions to account for imaging inconsistencies. Finally, the phase data from 1D Log-Gabor filters was extracted and quantized to four levels to encode the unique pattern of the iris into a bit-wise biometric template. The Hamming distance was employed for classification of iris templates, and two templates were found to match if a test of statistical independence was failed. The system performed with perfect recognition on a set of 756 eye images; however, tests on another set of 624 images resulted in false accept and false reject rates of 0.005% and 0.238% respectively. Therefore, iris recognition is shown to be a reliable and accurate biometric technology.***

Keywords: ***Automatic segmentation, Biometric identification, Iris recognition, Pattern recognition, etc.***

I. INTRODUCTION

The objective will be to implement an open-source iris recognition system in order to verify the claimed performance of the technology. The development tool used will be MATLAB, and emphasis will be only on the software for performing recognition, and not hardware for capturing an eye image. A rapid application development (RAD) approach will be employed in order to produce results quickly. MATLAB provides an excellent RAD environment, with its image processing toolbox, and high level programming methodology.

Manuscript published on 28 February 2012.
* Correspondence Author (s)
Ashish Kumar Dewangan*, M. Tech. Scholar (Digital Electronics), RCET, Bhilai, Chhattisgarh, India. 00919424132896. E-mail ID – ashishdewangan@csitdurg.in
Majid Ahmed Siddhiqui*, Department of electronics and telecommunication, RCET, Bhilai, Chhattisgarh, India. Email ID - majid.ece@gmail.com

To test the system, data sets of eye images will be used as inputs; a database of 756 grayscale eye images courtesy of The Chinese Academy of Sciences – Institute of Automation (CASIA) [6].The system is to be composed of a number of sub-systems, which correspond to each stage of iris recognition. These stages are segmentation – locating the iris region in an eye image, normalization – creating a dimensionally consistent representation of the iris region, and feature encoding – creating a template containing only the most discriminating features of the iris. The input to the system will be an eye image, and the output will be an iris template, which will provide a mathematical representation of the iris region.

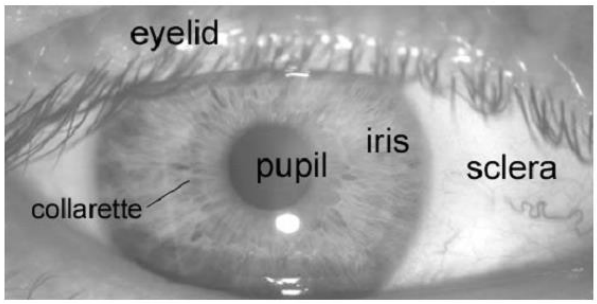

Figure-1 A front-on view of the human eye

II. METHODOLOGY

The first stage will be to develop an algorithm to automatically segment the iris region from an eye image. This will require research into many different techniques such as Daugman's integro-differential operator, circular Hough transform, and active contour models [18].Following this, the next stage will be to normalize the iris region in order to counteract imaging inconsistencies such as pupil dilation. An implementation of Daugman's polar representation [2] will be used for this purpose, as this is the most documented method for iris normalization. Once a normalized iris pattern has been obtained, it will be convolved with 2D Gabor wavelets in order to extract features.

This method is well documented in papers by Daugman [2], and also Boles [4] and a MATLAB function by Kovesi [10] is available to perform Gabor wavelet analysis. Finally, matching and statistical analysis will be performed in order to test how well iris patterns can be identified against a database of pre-registered iris patterns again this is well documented in the open literature. In the early stages of the project, the primary objective will be to get results. Once results are obtained and analyzed, the different parts of the software will be optimized, corrected and matching re-run.

This iterative cycle will

proceed until satisfactory results are obtained.

III. HOUGH TRANSFORM

The Hough transform is a standard computer vision algorithm that can be used to determine the parameters of simple geometric objects, such as lines and circles, present in an image. The circular Hough transform can be employed to deduce the radius and centre coordinates of the pupil and iris regions. An automatic segmentation algorithm based on the circular Hough transform is employed by Wildes et al. [3], Kong and Zhang [7], Tisse et al. [5], and Ma et al. [8]. Firstly, an edge map is generated by calculating the first derivatives of intensity values in an eye image and then thresholding the result. From the edge map, votes are cast in Hough space for the parameters of circles passing through each edge point. These parameters are the centre coordinates x_c and y_c, and the radius r, which are able to define any circle according to the equation

$$x_c^2 + y_c^2 - r^2 = 0$$

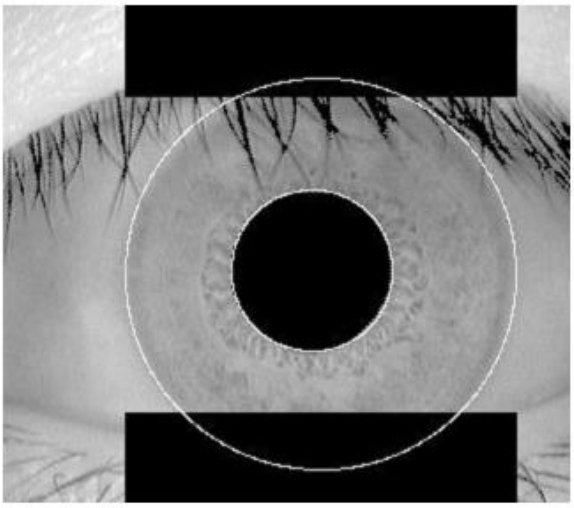

Figure-2 Segmented iris image.

A maximum point in the Hough space will correspond to the radius and centre coordinates of the circle best defined by the edge points. Wildes et al. and Kong and Zhang also make use of the parabolic Hough transform to detect the eyelids, approximating the upper and lower eyelids with parabolic arcs, which are represented as:

$$(-(x-h_j)\sin\theta_j + (y-k_j)\cos\theta_j)^2 = a_j((x-h_j)\cos\theta_j + (y-k_j)\sin\theta_j)$$

Where a_j controls the curvature, (h_j ,k_j is the peak of the

parabola and θ_j angle of rotation relative to the x-axis. In performing the preceding edge detection step, Wildes et al. bias the derivatives in the horizontal direction for detecting the eyelids, and in the vertical direction for detecting the outer circular boundary of the iris.

The motivation for this is that the eyelids are usually horizontally aligned, and also the eyelid edge map will corrupt the circular iris boundary edge map if using all gradient data. Taking only the vertical gradients for locating the iris boundary will reduce influence of the eyelids when performing circular Hough transform, and not all of the edge pixels defining the circle are required for successful localization. Not only does this make circle localization more accurate, it also makes it more efficient, since there are less edge points to cast votes in the Hough space.

IV. DAUGMAN'S RUBBER SHEET MODEL

The homogenous rubber sheet model devised by Daugman [1] remaps each point within the iris region to a pair of polar coordinates (r, θ) where r is on the interval [0, 1]

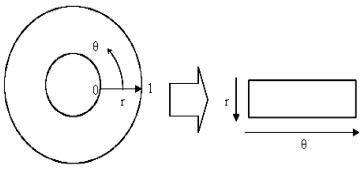

Figure-3 Daugman's rubber sheet model.

The remapping of the iris region from (x, y) Cartesian coordinates to the normalized non-concentric polar representation is modeled as

$$I(x(r,\theta), y(r,\theta)) \rightarrow I(r,\theta)$$

with

$$x(r,\theta) = (1-r)x_p(\theta) + rx_l(\theta)$$
$$y(r,\theta) = (1-r)y_p(\theta) + ry_l(\theta)$$

where $I(x, y)$ is the iris region image, (x, y) are the original Cartesian coordinates, (r, θ) are the corresponding normalized polar coordinates, and are the x_p , y_p x_l , y_l coordinates of the pupil and iris boundaries along the direction. The rubber sheet model takes into account pupil dilation and size inconsistencies in order to produce a normalized representation with constant dimensions. In this way the iris region is modeled as a flexible rubber sheet anchored at the iris boundary with the pupil centre as the reference point. Even though the homogenous rubber sheet model accounts for pupil dilation, imaging distance and non-concentric pupil displacement, it does not compensate for rotational inconsistencies.

In the Daugman system, rotation is accounted for during matching by shifting the iris templates in the direction until two iris templates are aligned.

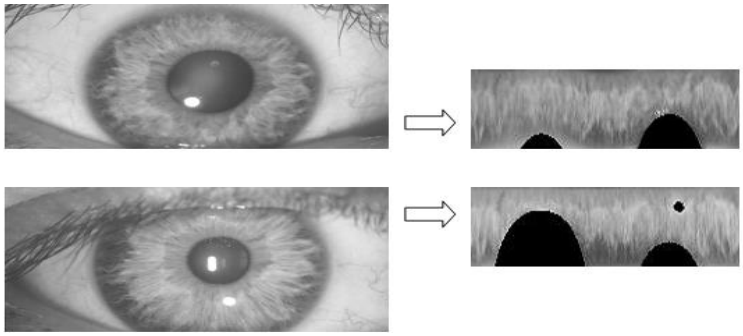

Figure-4 Normalised image.

Published By:
Blue Eyes Intelligence Engineering
and Sciences Publication (BEIESP)

V. LOG - GABOR FILTERS

A disadvantage of the Gabor filter is that the even symmetric filter will have a DC component whenever the bandwidth is larger than one octave [9]. However, zero DC components can be obtained for any bandwidth by using a Gabor filter which is Gaussian on a logarithmic scale; this is known as the Log-Gabor filter. The frequency response of a Log-Gabor filter is given as:

$$G(f) = \exp\left(\frac{-(\log(f/f_0))^2}{2(\log(\sigma/f_0))^2}\right)$$

Where f_0 represents the centre frequency and σ gives the bandwidth of the filter.

VI. MATCHING (HAMMING DISTANCE)

For matching, the Hamming distance was chosen as a metric for recognition, since bit-wise comparisons were necessary. The Hamming distance algorithm employed also incorporates noise masking, so that only significant bits are used in calculating the Hamming distance between two iris templates. Now when taking the Hamming distance, only those bits in the iris pattern that corresponds to '0' bits in noise masks of both iris patterns will be used in the calculation. The Hamming distance will be calculated using only the bits generated from the true iris region, and this modified Hamming distance formula is given as

$$HD = \frac{1}{N - \sum_{k=1}^{N} Xn_k(OR)Yn_k} \sum_{j=1}^{N} X_j(XOR)Y_j(AND)Xn'_j(AND)Yn'_j$$

Where Xj and Yj are the two bit-wise templates to compare, Xnj and Ynj are the corresponding noise masks for Xj and Yj, and N is the number of bits represented by each template. Although, in theory, two iris templates generated from the

same iris will have a Hamming distance of 0.0, in practice this will not occur. Normalisation is not perfect, and also there will be some noise that goes undetected, so some variation will be present when comparing two intra-class iris templates.

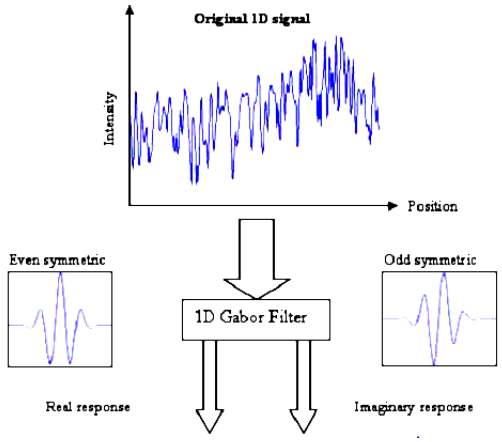

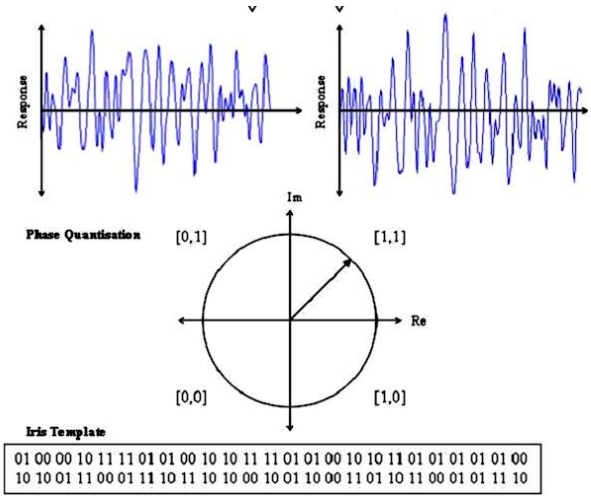

Figure -5 An illustration of the feature encoding process.

VII. MATCHING (HAMMING DISTANCE)

For matching, the Hamming distance was chosen as a metric for recognition, since bit-wise comparisons were necessary. The Hamming distance algorithm employed also incorporates noise masking, so that only significant bits are used in calculating the Hamming distance between two iris templates. Now when taking the Hamming distance, only those bits in the iris pattern that corresponds to '0' bits in noise masks of both iris patterns will be used in the calculation. The Hamming distance will be calculated using only the bits generated from the true iris region, and this modified Hamming distance formula is given as

$$HD = \frac{1}{N - \sum_{k=1}^{N} Xn_k(OR)Yn_k} \sum_{j=1}^{N} X_j(XOR)Y_j(AND)Xn'_j(AND)Yn'_j$$

Where Xj and Yj are the two bit-wise templates to compare, Xnj and Ynj are the corresponding noise masks for Xj and Yj, and N is the number of bits represented by each template. Although, in theory, two iris templates generated from the same iris will have a Hamming distance of 0.0, in practice this will not occur. Normalisation is not perfect, and also there will be some noise that goes undetected, so some variation will be present when comparing two intra-class iris templates.

In order to account for rotational inconsistencies, when the Hamming distance of two templates is calculated, one template is shifted left and right bit-wise and a number of Hamming distance values are calculated from successive shifts. This bit-wise shifting in the horizontal direction corresponds to rotation of the original iris region by an angle given by the angular resolution used. If an angular resolution of 180 is used, each shift will correspond to a rotation of 2 degrees in the iris region. This method is suggested by Daugman [1], and corrects for misalignments in the normalised iris pattern caused by rotational differences during imaging. From the calculated Hamming

Published By:
Blue Eyes Intelligence Engineering
and Sciences Publication (BEIESP)

distance values, only the lowest is taken, since this corresponds to the best match between two templates. The number of bits moved during each shift is given by two times the number of filters used, since each filter will generate two bits of information from one pixel of the normalised region. The actual number of shifts required to normalise rotational inconsistencies will be determined by the maximum angle difference between two images of the same eye, and one shift is defined as one shift to the left, followed by one shift to the right. The shifting process for one shift is illustrated in Figure.

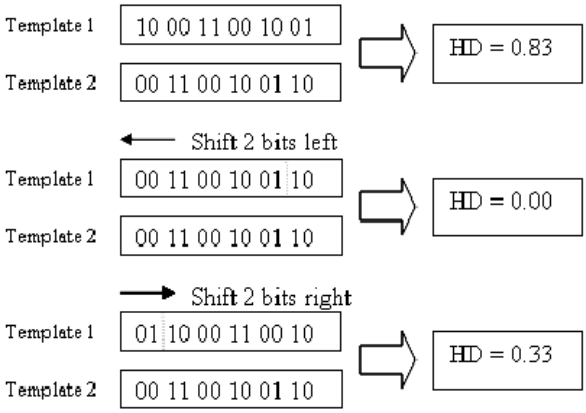

Figure-6 An illustration of the shifting process.

One shift is defined as one shift left, and one shift right of a reference template. In this example one filter is used to encode the templates, so only two bits are moved during a shift. The lowest Hamming distance, in this case zero, is then used since this corresponds to the best match between the two templates.

VIII. RESULT

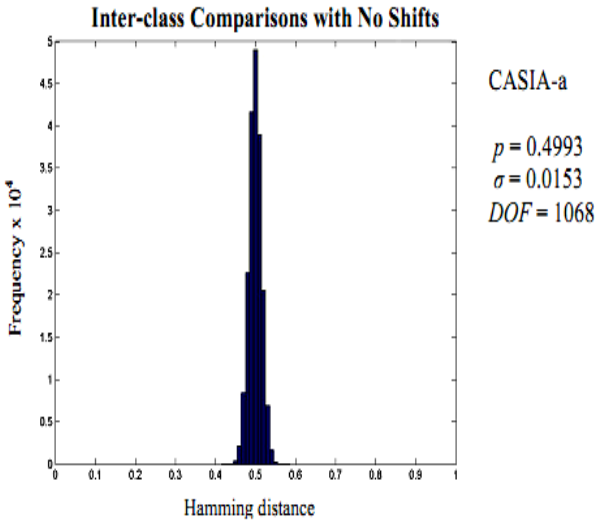

Figure-7 Inter-class Hamming distance distribution

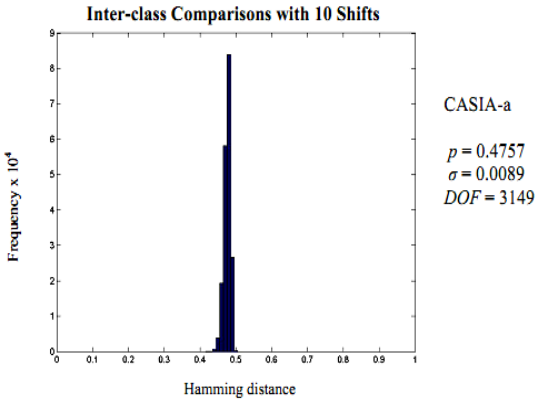

Figure-8 Inter-class Hamming distance distribution with 10 shifts left and right when comparing templates. Encoded with one filter.

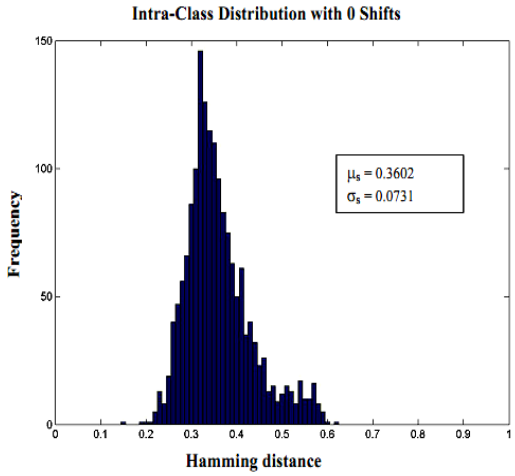

Figure-9 Intra class distribution with no shifts.

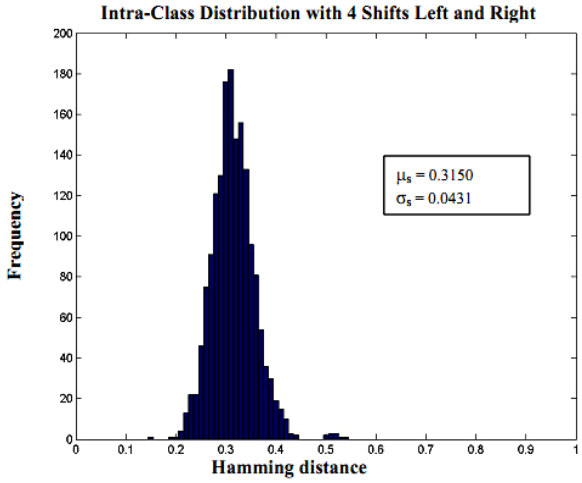

Figure-10 Intra-class distribution with 4 shifts left and right.

IX. CONCLUSION

Published By:
Blue Eyes Intelligence Engineering
and Sciences Publication (BEIESP)

As above figure shows, the inter-class Hamming distance distributions conform to the theory of statistical independence, since the mean of the distribution

equals 0.5. Therefore it can be stated that for 'CASIA-a', iris templates generated are highly unique, in that comparing any two templates generated from different irises is equivalent to comparing two random bit patterns. Also, the number of degrees calculated for data sets shows the complexity of the iris, with1068 degrees of freedom represented by the 'CASIA-a' data set.

Threshold	FAR (%)	FRR (%)
0.20	0.000	99.047
0.25	0.000	82.787
0.30	0.000	37.880
0.35	0.000	5.181
0.40	0.005	0.238
0.45	7.599	0.000
0.50	99.499	0.000

Table1-False accept and false reject rates for the 'CASIA-a' data set with different separation points using the optimum parameters.

As shifting was introduced, so that intra-class templates were properly lined up, the mean inter-class Hamming distance value decreased as expected. With 10 shifts the mean decreased to 0.47 for both as shown in Figure. The standard deviation of inter-class distribution was also reduced, this was because the lowest value from a collection was selected, which reduced outliers and spurious values. The shifting also caused a reduction in the number of degrees of freedom, DOF. This reduction in DOF is an anomaly caused by a smaller standard deviation, which itself is caused by taking the lowest Hamming distance from 10 calculated values. This shows that, due to shifting, the distribution is not merely shifted towards the left, but the characteristics of the distribution are changed. Therefore the degrees of freedom formula is not very useful with shifting introduced, since it relies on the distribution approximating a binomial.

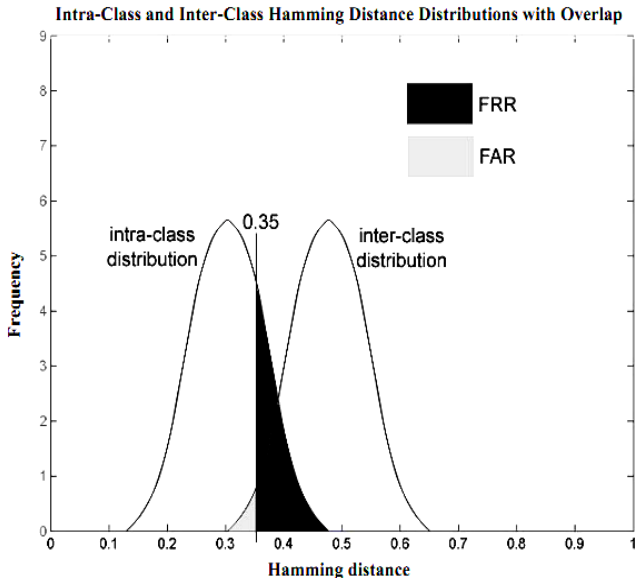

Figure-11 False Accept and False Reject Rates for two distributions with a separation Hamming distance of 0.35.

REFERENCES

1. S. Sanderson, J. Erbetta. Authentication for secure environments based on iris scanning technology. IEEE Colloquium on Visual Biometrics, 2000.
2. J. Daugman. How iris recognition works. Proceedings of 2002 International Conference on Image Processing, Vol. 1, 2002.
3. R. Wildes, J. Asmuth, G. Green, S. Hsu, R. Kolczynski, J. Matey, S. McBride. A system for automated iris recognition. Proceedings IEEE Workshop on Applications of Computer Vision, Sarasota, FL, pp. 121-128, 1994.
4. W. Boles, B. Boashash. A human identification technique using images of the iris and wavelet transform. IEEE Transactions on Signal Processing, Vol. 46, No. 4, 1998.
5. C. Tisse, L. Martin, L. Torres, M. Robert. Person identification technique using human iris recognition. International Conference on Vision Interface, Canada, 2002.
6. Chinese Academy of Sciences – Institute of Automation. Database of 756 Greyscale Eye Images. http://www.sinobiometrics.com Version 1.0, 2003.
7. W. Kong, D. Zhang. Accurate iris segmentation based on novel reflection and eyelash detection model. Proceedings of 2001 International Symposium on Intelligent Multimedia, Video and Speech Processing, Hong Kong, 2001.
8. L. Ma, Y. Wang, T. Tan. Iris recognition using circular symmetric filters. National Laboratory of Pattern Recognition, Institute of Automation, Chinese Academy of Sciences, 2002.
9. D. Field. Relations between the statistics of natural images and the response properties of cortical cells. Journal of the Optical Society of America, 1987.
10. P. Kovesi. MATLAB Functions for Computer Vision and Image Analys is. Available at: http://www.cs.uwa.edu.au/~pk/Research/MatlabFns/index.html

Published By:
Blue Eyes Intelligence Engineering
and Sciences Publication (BEIESP)